Electrochemical and Spectroelectrochemical Behavior of a Tetracyanotriphenodioxazine in Solution and Thin-Films

Rita Meunier-Prest, Guillaume Gruntz, Frédéric Castet, Yohann Nicolas, Amélie Wannebroucq, Marcel Bouvet, Thierry Toupance

Graphical Abstract

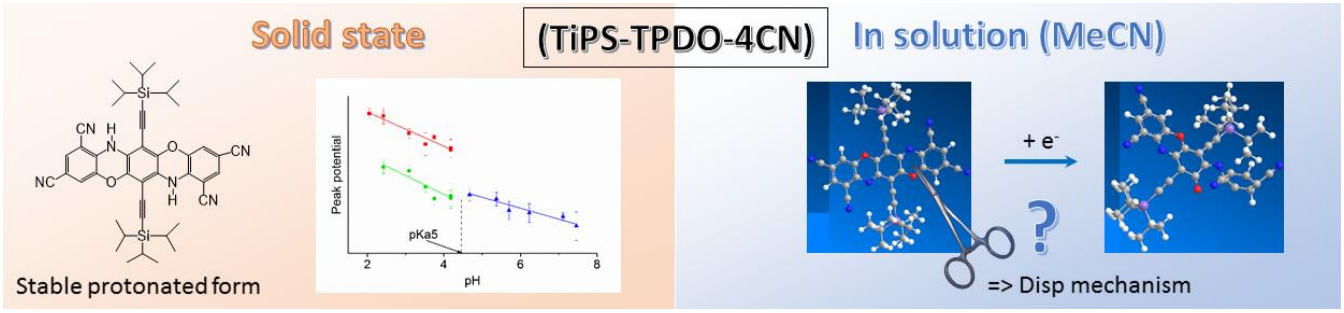

Change of state, change in behavior. The protonated form of TiPS-TPDO-tetraCN is stable in the solid-state and follows a classical square scheme reaction whereas in solution, it is unstable. In organic solvents, TiPS-TPDO-tetraCN reduction involves two $1e^-$ steps in CH_2Cl_2 while in acetonitrile, the electron transfer induces structural changes, such as break of bonds, that promote the DISP mechanism.

Electrochemical and spectroelectrochemical behaviors of a tetracyanotriphenodioxazine bearing two triisopropylsilylethynyl moieties (TiPS-TPDO-tetraCN) in solution and thin films

Rita Meunier-Prest,*[a] Guillaume Gruntz,[b] Frédéric Castet,[b] Yohann Nicolas,*[b] Amélie Wannebroucq,[a] Marcel Bouvet,[a] and Thierry Toupance[b]

Abstract: We report the electrochemical behavior of TiPS-TPDO-tetraCN during its reduction studied either in solution or after vacuum evaporation deposition on ITO. While in dichloromethane it typically proceeds in two successive monoelectronic reactions, in acetonitrile, the mechanism appears more complex. Fine analysis of the spectroelectrochemical results combined with simulation of the voltammograms with various amount of water suggest the involvement of water and of a restructured dianion in the electrochemical process. In the solid-state, the formation of the diprotonated compound was demonstrated and the equilibrium diagram of the different species formed as a function of the pH was drawn. The deprotonated form is unstable and decomposes immediately in solution. Its stabilization in the solid-state is attributed to π–π and charge transfer interactions.

Introduction

Recent research efforts in the field of electron-poor π-conjugated compounds mainly concerns n-type organic semiconductors (OSC) which are combined with p-type materials in heterojunctions. Whereas the latter afforded high performances in many different electronic devices, n-type OSCs still remain rare for numerous applications. Thus, most of studies on organic photovoltaic devices bring into play fullerene derivatives as n-type active OSCs. On the other hand, the development of new n-type OSCs is driven by the possibility in organic electronics to build complementary circuits, with the ability to switch organic field-effect transistors (OFET) with both positive and negative gate voltages[1], as it has been already achieved with inorganic materials in complementary metal-oxide-semiconductors (CMOS). To design an efficient n-type OSC for these devices, the stabilization of its anionic form is required. Indeed the reduced form of the material, which bears the charge carrier, should not react chemically with its environment or with itself. A solution consists in shifting the reduction potential towards less negative values to obtain less reactive anions. Thus, the introduction of electron-withdrawing substituents on aromatic cores leads to more stable charge carriers by lowering the energy of the π-delocalized Lower Unoccupied Molecular Orbital (LUMO) and increasing the reduction potential. For example, fluoro or cyano substituents introduced on a phthalocyanine ring[2] or on oligothiophenes[3] stabilize the reduced states as well as carbonyl groups in perylene.[4] Another way to transform a p-type material into a n-type analogue is to introduce nitrogen instead of carbon atoms directly inside the aromatic core. Thus, whereas pentacene exhibits a p-type behavior, tetraazapentacenes that contain four nitrogen yield efficient n-type OSCs.[5] Similarly, triphenodioxazines (TPDO) containing nitrogen and oxygen atoms and endowed with cyano groups afforded stable n-type OFETs.[6] Additionally, the quinonoid structure at the center of the pentacycle in TPDOs is responsible for enhancing the stability of their anionic form.[7]

Recently, we extended their potentialities of n-type OSCs to another organic electronic device - the conductometric chemical sensors.[8] Thus, we reported a new class of n-type sublayer in Molecular Semiconductor - Doped Insulator heterojunctions (MSDI)[8] made of a tetracyano triphenodioxazine bearing two triisopropylsilylethynyl moieties (TiPS-TPDO-tetraCN), combined with a highly conductive molecular material, the lutetium bisphthalocyanine, $LuPc_2$. In the course of this investigation, an unexpected behavior was highlighted. When the devices were prepared by vacuum evaporation of TiPS-TPDO-tetraCN, a high and competitive MSDI chemical sensor was obtained in contrast to devices processed by spin-coating. We demonstrated that it was due to the formation of the diprotonated molecule during the vacuum evaporation process. However, in the triphenodioxazine series, only few examples of diprotonated structures were reported[9] and no data about their redox properties.

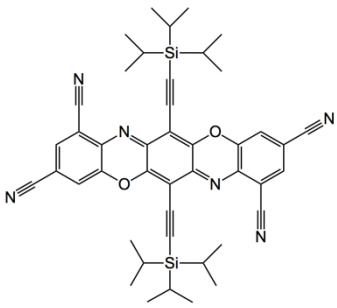

Scheme 1. Schematic view of the TIPS-tetracyano- triphenodioxazine (TiPS-TPDO-tetraCN)

Taking into account the quinonediimine structure of TPDOs, it is worth reminding the electrochemical behavior of para-benzoquinones to understand this of TPDOs. Due to their

[a] Dr. R. Meunier-Prest, A. Wannebroucq and Pr. M. Bouvet
Institut de Chimie Moléculaire de l'Université de Bourgogne (ICMUB), UMR 6302, CNRS, Université Bourgogne Franche-Comté, 9 avenue Alain Savary, 21078 Dijon Cedex, France.
E-mail: rita.meunier-prest@u-bourgogne.fr
[b] Dr. Guillaume Gruntz, Dr. Frédéric Castet, Dr. Yohann Nicolas and Pr. Thierry Toupance
C2M - ISM - Université de Bordeaux, 351 cours de la libération, 33405 Talence Cedex, France
E-mail: Yohann.Nicolas@enscbp.fr

important role in biological processes,[10] quinones have been widely studied. It is well-known that benzoquinones (BQ) can be reduced into dihydroquinones (H_2Q), but the involved mechanisms and thermodynamics depend on the quinones environment. Thus, a molecule adsorbed on a working electrode exhibits electrochemical processes different from these of molecules in solution, due to intermolecular interactions and solvation energies. When the quinones are incorporated into a self-assembled monolayer, the global two electrons – two protons electrochemical reduction, in aqueous media, can be described on the basis of a nine-member square scheme.[11] However, the reaction proceeds through proton-coupled electron transfer in aqueous media,[12] but not in unbuffered media.[13] In the solid-state, in addition to the reduced and oxidized forms, another structure, called quinhydrone, can be stabilized, which combines both redox species. Quinhydrones are well-known charge transfer complex between the electron-acceptor (BQ) and the electron-donor (H_2Q) π systems. They are stabilized by π–π interactions inside the donor-acceptor stacks while infinite molecular chains formed through hydrogen bonds between neighboring columns.[14]

To get a deeper insight in the chemical structure and the formation mechanism of the diprotonated TiPS-TPDO derivative during the vacuum evaporation of TiPS-TPDO-tetraCN and in the redox properties of thin films used in MSDI devices, we hereafter report on its electrochemical reduction behavior both in solution and solid-state. In particular, a spectroelectrochemical study was carried out in acetonitrile solutions, with and without water, followed by simulations of the voltammograms, to characterize the different reduced species, to study the reversibility of the electrochemical reaction and to better understand the reaction mechanism. The key point was to identify if the diprotonated species was also formed in solution. Finally, to highlight the role of protons, electrochemical responses of films prepared by vacuum evaporation of TiPS-TPDO-tetraCN onto ITO substrates were recorded in aqueous medium.

Results and Discussion

TIPS-TPDO-tetraCN in solution

Electrochemical behavior of TiPS-TPDO-tetraCN in CH_2Cl_2. The cyclic voltammogram of TiPS-TPDO-tetraCN recorded in dichloromethane (CH_2Cl_2) (Fig. 1) presented two quasi-reversible reduction steps at – 185 mV and – 618 mV / SCE with a difference between anodic and cathodic peak potentials larger (ΔEp = 100 mV) than what it was theoretically expected (58 mV), due to the resistivity of the medium. For both systems, the ratio of the anodic to cathodic peak currents was equal to one and the voltammogram recorded on ultramicroelectrode, under stationary conditions, showed two waves of equal intensity each one corresponding to the transfer of one electron. It matches the following EE mechanism leading first, to the radical anion and then to the dianion ($\boldsymbol{E_2^0 < E_1^0}$).

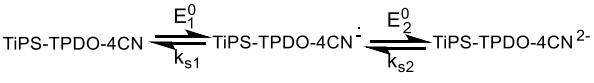

(1)

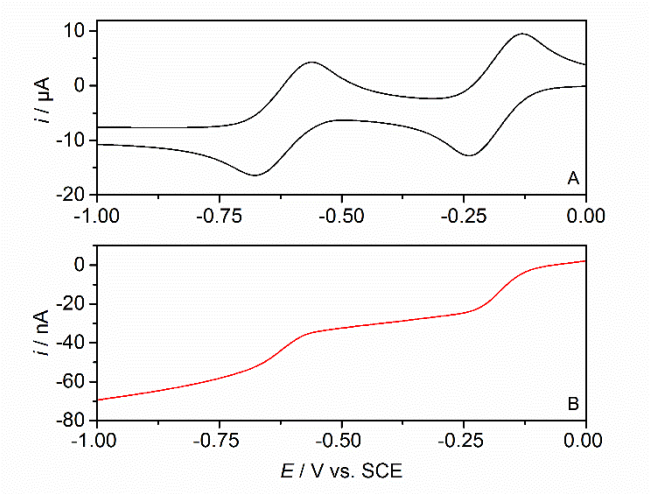

Figure 1. Voltammograms of TiPS-TPDO-tetraCN 1.9x10^{-3} M in CH_2Cl_2 + Bu_4NPF_6 0.1 M: A, on a Pt disk electrode (diameter 1.6 mm) at a scan rate of 100 mV s^{-1} and B, on an ultramicroelectrode of 50 µm at a scan rate of 40 mV s^{-1}.

Electrochemical behavior of TiPS-TPDO-tetraCN in MeCN. In acetonitrile, the electrochemical behavior was slightly different. Both reduction steps were still observed. The systems were fully reversible (ΔEp = 58 mV) with a little offset more positive potentials (E^0_1 = – 112 mV and E^0_2 = – 487 mV) compared to those obtained in CH_2Cl_2. The difference between both redox systems, ($E^0_1 - E^0_2$), was smaller (375 mV) than that observed in CH_2Cl_2 (433 mV). This difference depends on many factors such as delocalized or localized charge in the ions, ion pairing with the supporting electrolyte, structure of the molecule (linear, presence of unsaturated bonds or aromaticity)[15] and also the nature of the solvent.[16] In particular, it has been shown that this difference ($E^0_1 - E^0_2$) increases with decreasing the solvent polarity,[16] as we have observed when switching solvent from acetonitrile to dichloromethane. In the present case, peak currents varied linearly with $v^{1/2}$ indicating that the reaction is diffusion controlled. Another difference appeared on the second reduction system where the cathodic peak (E_{pc2}) was smaller than the first one and was preceded by a small shoulder (E_{pcw}). The explanation for this shoulder was partly provided by the same study in presence of water (Fig. 2). When increasing amounts of water were added, evolution of the second system was observed: the anodic peak (E_{pa2}) decreased while the cathodic one was shifted towards positive values up to the potential corresponding to the shoulder, at - 450 mV (E_{pcw}), which grew with the increasing concentration of water. The figure 2B shows the evolution of the cathodic peak potentials as a function of the logarithm of the water concentration.

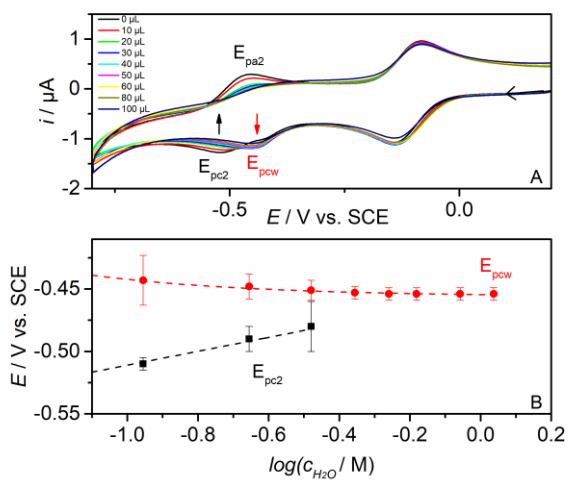

Figure 2. A, evolution of the voltammograms of TiPS-TPDO-tetraCN 2.10^{-4} M in MeCN + Bu_4NPF_6 0.1 M, on a Pt disk electrode (diameter 1.6 mm) at a scan rate of 100 mV s^{-1}, when increasing amounts of water are introduced into the cell (5 ml of solution) and B, cathodic peak potentials of the second reduction step as a function of the logarithm of the concentration of water added to the solution.

As it was evidenced in the reduction mechanism of quinones, this potential displacement can be assigned to fast hydrogen-bonding equilibria[17] inducing stabilization of the dianion by water molecules. Finally, a last difference has been observed. While both redox systems had the same intensity in CH_2Cl_2, the second system was smaller than the first one in MeCN. Consequently, a more complex mechanism should occur that consumes part of the radical anion and provides the initial product back. To investigate more deeply this mechanism, a spectroelectrochemical study was conducted.

Spectroelectrochemistry of TiPS-TPDO-tetraCN in MeCN. The UV-visible spectrum of TiPS-TPDO-tetraCN in acetonitrile (Fig. 3 before electrolysis) was first recorded and exhibited two maxima at 554 and 522 nm and a shoulder at 484 nm (Table 1). The absorption spectrum simulated using time-dependent density functional theory (TD-DFT) at the M06-2X/6-311+G(d) level (see the computational section for details) is provided in supporting information (Fig. S1), as well as the shape of the frontier molecular orbitals and the electron density difference between the ground state and the lowest-energy excited state (Fig. S2). As shown in the computed spectrum, the first absorption band, which is attributed to a HOMO-to-LUMO electronic excitation, is red-shifted by 44 nm (0.16 eV) compared to experiments.

Table 1. Absorption bands of TiPS-TPDO-tetraCN in acetonitrile

λ_{max} (nm)	484 (sh.)	522	554
ε (M^{-1} cm^{-1})	3300	6200	6600

Then, an electrolysis of TiPS-TPDO-tetraCN (10^{-3} M) was performed to determine the number of electrons involved in the global reduction process. A potential of – 0.6 V was imposed, i.e. after the second reduction step (Fig. 2). After consumption of 2 electrons per molecule of TiPS-TPDO-tetraCN, the current decreased to zero and the electrolysis was stopped (96 mC) as expected from earlier studies. This confirms the involvement of 2 electrons in the global reduction step.

To get an insight on the nature of the reduced species and on the reversibility of the electrochemical reaction, we then carried out two spectroelectrochemical experiments on the solution of neutral TIPS-TPDO-TetraCN. In the first one, we imposed a potential of –0.2 V corresponding to the first reduction step. After consumption of 48 mC corresponding to an exchange of one electron per molecule, i.e. half of the amount of electricity consumed at – 0.6 V, the experiment was stopped. It took 1800s. The progress of the electrolysis was followed by UV-visible spectroscopy (one spectrum every 6 s, i.e. 300 spectra). Fig. 3A presents the evolution of the spectra. The absorption bands of TiPS-TPDO-tetraCN at 484, 522 and 554 nm decreased while new absorption bands at 628 and 680 nm appeared. It is important to note that after consumption of one electron per molecule, half of the initial amount of TiPS-TPDO-tetraCN remained present in the cell. This topic will be addressed in details in the paragraph “Discussion on the reduction mechanism in acetonitrile”.

In the second spectroelectrochemical experiment, we imposed a potential of -0.6 V corresponding to the second reduction step. The experiment was stopped when the current tended to zero, after 3600 s and consumption of 96 mC. The consumption of two electrons per molecule of TiPS-TPDO-tetraCN led to complete disappearance of the absorption bands of the initial product (Fig 3B). At the same time, three absorption bands at 574, 628 and 680 nm (Table 2) grew rapidly.

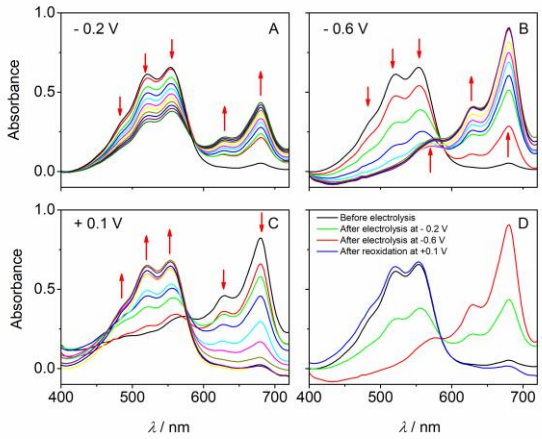

Figure 3. Spectroelectrochemical experiments performed on 10^{-3} M TiPS-TPDO-tetraCN in MeCN + Bu_4NPF_6 0.1 M at (A) - 0.2 V during 1800 s, (B) - 0.6. V during 3600 s, (C) after reoxidation at + 0.1 V and (D) comparison of the last spectrum of each electrolysis with the initial spectrum.

Table 2. Absorption bands of the dianionic species obtained after 2e⁻ electrolysis in acetonitrile

λ_{max} (nm)	574	628	680
ε (M^{-1} cm^{-1})	2000	4000	9000

Moreover, the spectra showed an isosbestic point at 586 nm, which reveals the existence of only two chromophores in the solution. The reaction is perfectly reversible since the spectroelectrochemical reoxidation of this solution at + 0.1 V gave back to the absorbance spectrum of TiPS-TPDO-tetraCN (Fig. 3C-D) with the same intensity as that of the initial product. At a first glance, we assigned the new absorption bands emerging at large wavelengths to the $(TiPS\text{-}TPDO\text{-}tetraCN)^{2-}$ dianion, which is the expected reduced species in organic solvent. However, this assumption was contradicted by TDDFT calculations, which evidenced that the 2e- electrolysis of TiPS-TPDO-tetraCN should give rise to blue shift of 23 nm (0.08 eV) of the absorption maximum (Fig. S1), instead of the red shift observed experimentally. It must be also pointed out that, on the time scale of the spectroelectrochemical experiment, the formed dianionic species remains perfectly stable.

In light of these results, the spectrum obtained after one electron reduction per molecule at –0.2 V corresponds to the superimposition of the spectrum of the initial compound, TiPS-TPDO-tetraCN and of a 2e⁻ reduction product, different from $(TiPS\text{-}TPDO\text{-}tetraCN)^{2-}$. To rationalize this finding, the existence of a chemical reaction involving the radical anion $(TiPS\text{-}TPDO\text{-}tetraCN)^{\bullet-}$ and leading to TiPS-TPDO-tetraCN and a dianionic compound should be considered. Since $E_2^0 < E_1^0$ (eq.1) and owing to the computational results, a disproportionation (DISP) mechanism can be ruled out.[18] To check the involvement of the radical anion in the formation of TiPS-TPDO-tetraCN and dianion, a spectroelectrochemical experiment at -0.2 V in the presence of (2,2,6,6-Tetramethylpiperidin-1-yl)oxyl (TEMPO) – a radical scavenger[19] –, was performed. First, the absorption spectrum and the cyclic voltammogram of TEMPO were recorded to ensure that its responses were out of the range studied in our experimental conditions. Actually, the UV-visible spectrum presented one band at 254 nm and a weak band at 640 nm and the voltammogram showed only a redox system at 0.6 V / SCE. Fig. 4 depicts the evolution of the absorption spectra during the spectroelectrochemistry in the presence of an excess of TEMPO (C_{TEMPO} = 5 x $C_{TiPS\text{-}TPDO\text{-}tetraCN}$). In this region, the absorption of TEMPO was negligible compared to this of TPDO derivatives.

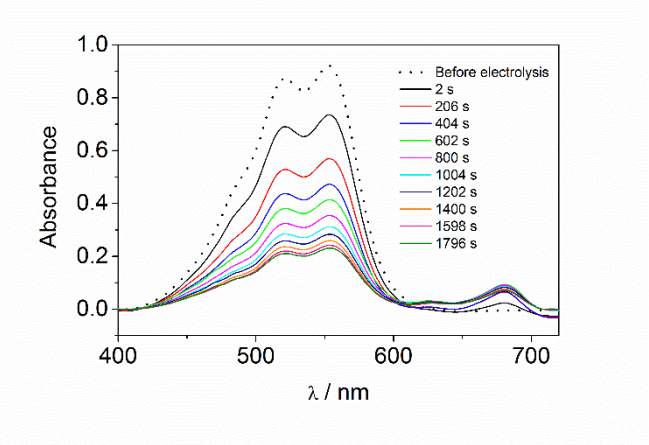

Figure 4. Spectroelectrochemical experiments performed on 10^{-3} M TiPS-TPDO-tetraCN in MeCN + Bu_4NPF_6 0.1 M in presence of $5x10^{-3}$ M TEMPO.

A decrease of the absorption bands corresponding to TiPS-TPDO-tetraCN was observed as above. But, contrary to the experiment in the absence of TEMPO, there was almost no emergence of the bands at 628 and 680 nm. This confirms the key role of the radical anion $(TiPS\text{-}TPDO\text{-}tetraCN)^{\bullet-}$ in the chemical process. The very small band at 680 nm is probably due to a competition between this chemical reaction and the trapping of the radical anion by TEMPO.

Spectroelectrochemistry of TiPS-TPDO-tetraCN in presence of water. The spectroelectrochemical experiment of TiPS-TPDO-tetraCN was repeated in acetonitrile containing 2% H_2O v/v i.e. $c_{H_2O} = 1\ M$ as previously done for cyclic voltammetry. This corresponds to the addition of 100 µl of water in the experiment of Fig. 2. The evolution of the absorption spectra was similar to that observed in absence of water. The only difference is the position of the shoulder at 574 nm that is slightly shifted to 564 nm in presence of water. It should be noted that the UV-visible spectrum at the end of the electrolysis remained the same as without water and still was different from that of the diprotonated compound $(TiPS\text{-}TPDO\text{-}tetraCN)H_2$.[8-9] It corresponded only to that of the dianionic compound (Fig. 3 and Table 2). Kinetics of formation and disappearance of the different products were measured according to the potential imposed during the electrolysis. Therefore, the absorbance at 522 nm and 680 nm was monitored to follow the concentration of TiPS-TPDO-tetraCN and this of the dianionic product, respectively (Fig. 5). The band at 522 nm was preferred to that at 554 nm to avoid the absorption spectra's overlap of TiPS-TPDO-tetraCN and the new dianionic species. During the electrolysis at - 0.6 V, absorbance at 522 nm (Fig. 5A) decreased until a value of 0.1, which corresponds to the foot of the band at 564 nm due to the formation of the dianion. Reoxidation of the solution led back to the initial concentration in TiPS-TPDO-tetraCN (Absorbance of 0.44).

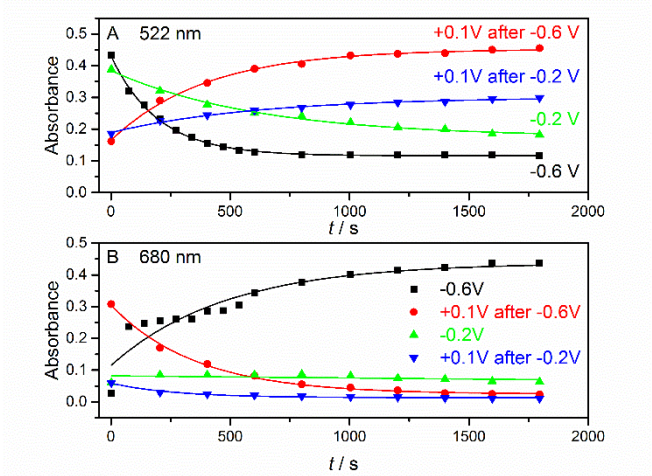

Figure 5. Evolution of the absorbance of bands at: A. 522 nm and B. 680 nm, during the different spectroelectrochemical experiments in the presence of 2% H_2O (1 M). The imposed electrolysis potentials are indicated on the graph.

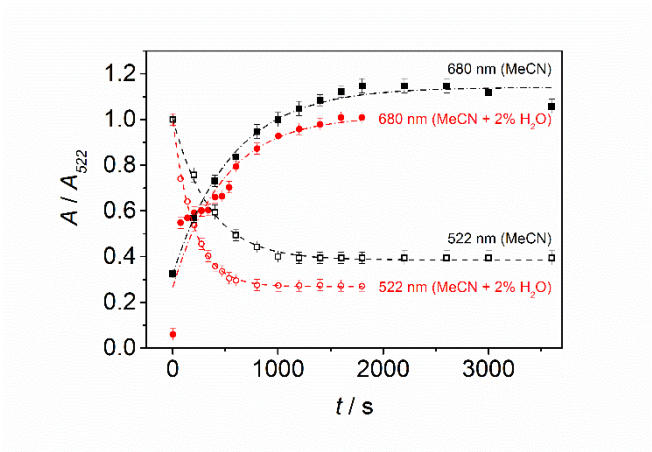

Figure 6. Comparison of the kinetics of appearance of the dianion (band at 680 nm) and disappearance of TiPS-TPDO-tetraCN (band at 522 nm) in absence and in presence of water during electrolysis at -0.6 V

At the same time, absorbance at 680 nm grew rapidly and disappeared during reoxidation (Fig. 5B). Both kinetic curves of absorbance of the band at 522 nm during electrolysis at + 0.1 V (Fig. 5A) and that at 680 nm during electrolysis at - 0.6 V (Fig. 5B) exhibited the same shape, which shows the perfect reversibility of the reaction. However, when a potential of -0.2 V was imposed, the absorbance at 680 nm remained very low and did not increase contrary to that was obtained in the absence of water (Fig. 3). Reoxidation of the solution gave back only partially the initial product.

Comparison of kinetics at – 0.6 V in absence and in presence of water was performed and the results are shown in Fig. 6. The small differences in concentration of TiPS-TPDO-tetraCN across the different experiments carried out have induced small differences in absorbance. In order to correct these differences, we divided all the absorbances of a same experiment by that of the band at 522 nm in the initial spectrum (A_{522}).

Fig. 6 shows the presence of water did not affect kinetics of formation of the dianion (band at 680 nm) while kinetics of disappearance of TiPS-TPDO-tetraCN was much faster in presence of water.

Discussion on the reduction mechanism in acetonitrile. The above results revealed the main features on the reduction mechanism of TiPS-TPDO-tetraCN in acetonitrile: it is reduced in two successive one-electron steps (Eq. 1 with $E^0_1 > E^0_2$), the second system being smaller than the first one, as shown by cyclic voltammetry. A 1 e^- per molecule electrolysis, at – 0.2 V (first reduction step (E_1^0)), has led to half of the initial concentration in TiPS-TPDO-tetraCN and dianionic compound as shown by spectroelectrochemical studies. The same experiment performed in presence of a radical scavenger, no longer leads to TiPS-TPDO-tetraCN and the dianionic product. The existence of a chemical reaction involving the radical anion $(TiPS\text{-}TPDO\text{-}tetraCN)^{\cdot-}$ and leading to TiPS-TPDO-tetraCN and an unknown dianionic compound must be considered. It cannot be a disproportionation mechanism (DISP) corresponding to the homogeneous electron transfer reaction that, from B, gives back to A and C because $\boldsymbol{E_2^0 < E_1^0}$).[18] Similarly, dimerization is not foreseeable because it is a 0.5 e^- process. Therefore, a more complex process that consumes part of the radical anion and gives the initial product back must be envisaged. Let us consider a mechanism (bottom rectangle in scheme 2) where the radical anion $(TiPS\text{-}TPDO\text{-}tetraCN)^{\cdot-}$ (B in scheme 2) and the dianion $TiPS\text{-}TPDO\text{-}tetraCN^{2-}$ (C in scheme 2) are both involved in first order reactions such as rearrangement, ring opening, ring reorganization or conformation changes.

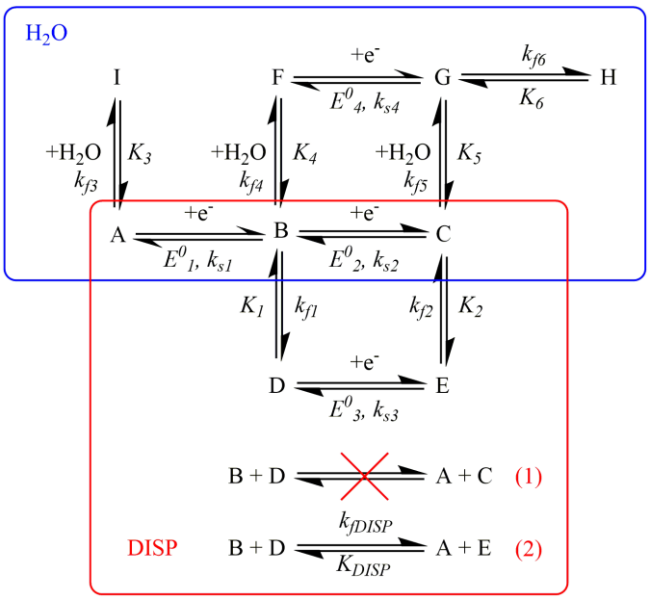

Scheme 2. The DISP mechanism. Bottom (circled in red): Disp mechanism; top (circled in blue): mechanism involving water molecules.

For example, planar and rigid π-conjugated systems with a pentacene like frame where two aromatic rings containing nitrogen atoms and having vicinal disubstitution of aryl/aryl groups undergo a cleavage of the N/aryl bond that leads to non-planar molecules.[20] A second example is that of quinacridone analogues, which exhibit conformation dynamic changes triggered electrochemically.[21] Structural changes accompanying electron transfer have already been reported to render disproportionation (DISP) to be less unfavorable.[22] They could occur as a chemical reaction preceding or following the electron transfer. Due to the delocalization of negative charges bore by the nitrogen atoms till the cyano moieties in ortho and para positions, the reduction of TIPS-TPDO-tetraCN (A in scheme 3) leads to chemical structures negatively charged on these atoms, as exemplified by the 2e$^-$ reduced TIPS-TPDO-tetzraCN^{2-} (C in scheme 3). Let us consider chemical structures compatible with such a DISP mechanism. At first, it is worth mentioning that diarylamino-1,4-benzoquinone can be chemically oxidized into dioxazine derivatives (Scheme 4).[23] Thus, such a quinone structure could be assumed as the result of the reduction of TiPS-TPDO-tetraCN (A). However, it requires breaking simultaneously two chemical bonds, which is generally not kinetically favored. But, starting from the doubly reduced TiPS-TPDO-tetraCN^{2-} (C), it is possible to write a mesomeric form that involves a 1,2-benzoquinone – like structure (E in scheme 3), which necessitates to break only one chemical bond. In a similar way, such orthoquinone structure (D) can be obtained by rearrangement, from the 1e$^-$ reduced (TiPS-TPDO-tetraCN)$^{\cdot-}$. Its 1e$^-$ reduction (E^0_3) leads to the 1,2-benzoquinone – like dianion (E in scheme 3). The structures (D) and (E) are proposed here as examples of restructured species to illustrate the phenomena observed in the spectroelectrochemical experiment.

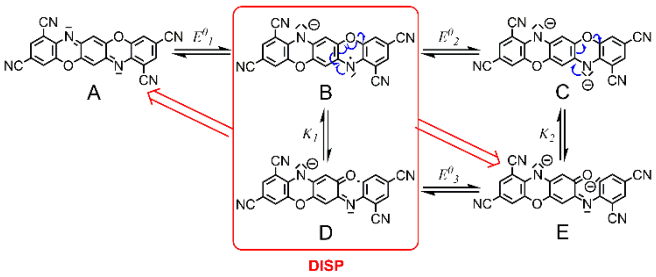

Scheme 3. Various possible intermediates involved in the DISP mechanism. For sake of clarity, the TIPS groups have been omitted and the non bonding electron pairs are only shown on the atoms involved in the process.[23]

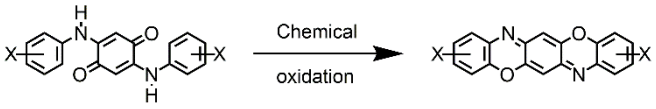

Scheme 4. Chemical oxidation of diarylamino-1,4-benzoquinone into dioxazine derivatives.[23]

The existence of this dynamic changes triggered electrochemically could induce the regeneration of the initial product, A, by two new DISP pathways (Bottom rectangle in scheme 2). Both are homogeneous electron transfer reactions of B and D to form respectively A and C (reaction (1)) or A and E (reaction (2)). After solving the system equations, the disproportionation constant of reaction (1) remains too small to bring back to TiPS-TPDO-tetraCN in such a large proportion as in the spectroelectrochemical experiments. Another possibility consists in reaction (2) of scheme 2 involving the radical anions, B and D that disproportionate into the initial product, A, and the compound E, obtained after modification of the dianion. It occurs only if E^0_3 is higher than E^0_1 and E^0_2. As indicated in Scheme 2, disproportionation of B and D leads to the regeneration of A and to the 2e$^-$ reduced form E. This balance equation occurs with no modification of the number of bonds, while rupture/creation of bonds takes place during the rearrangement of B in D (scheme 3).

We decided to simulate this mechanism to check if it could explain the smaller intensity of the second system compared to that of the first one in the cyclic voltammetry study. At the same time, influence of addition of water on the evolution of the second system has also to be taken into account in the global mechanism (Top rectangle in scheme 2). Indeed, the anodic peak decreased while the cathodic one was shifted towards positive values up to the potential corresponding to the shoulder, at - 450 mV. Such a behavior was already reported when quinones are reduced in the presence of water: Quan et al[17e] emphasized the role of hydrogen bonding between water molecules and the dianion that was stated to exist as a mixture of various proton states due to its acid-base properties. F and G correspond to complexes of radical anions, B, and dianions, C, with water molecules. The radical anion complex is more easily reduced than the non-complexed species and its potential E^0_4 is related to E^0_2, K_4 and K_5. When a relatively large concentration of water (c_{H2O} > 0.8 M i.e. when the amount of water is higher than 80 µL in Fig. 2) is introduced in the cell, partial destruction of TiPS-TPDO-tetraCN was observed. Reactions $A \leftrightarrow I$ and $G \leftrightarrow H$ were introduced to reflect this phenomenon. It should be noted that neither the DISP mechanism (red bottom rectangle in scheme ~~5~~2) nor the mechanism involving reactions with water (top blue rectangle in scheme 2~~5~~) can alone reflect the experimental results. The global mechanism in scheme 2 need to be considered to fit properly the experimental voltammograms. In particular, if the DISP mechanism is omitted, the anodic peaks decreased too much when the concentration in water was increased and, on the other hand, if the mechanism caused by water is missed, the potential shift obtained when increasing water concentration cannot be observed. The description of the approach used during the digital simulations was presented in the supporting information.

The comparison between experimental and simulated curves is presented in Fig.7 for two different concentrations in water (1 M and 2 M). All the parameters are the same in both simulations except the water concentration. When possible, the values entered in the simulations, such as E^0_1 and E^0_2, are derived from

experimental data. Other constants were adjusted by fitting related parameters, for example, E^0_4 was adjusted by fitting the equilibrium constants K_4 and K_5.

The good agreement between experimental and simulated curves in the presence of H_2O strongly supports the formation of complexes with water in anion stabilization and of the involvement of structural changes accompanying electron transfer that make disproportionation (DISP) to be more favorable.

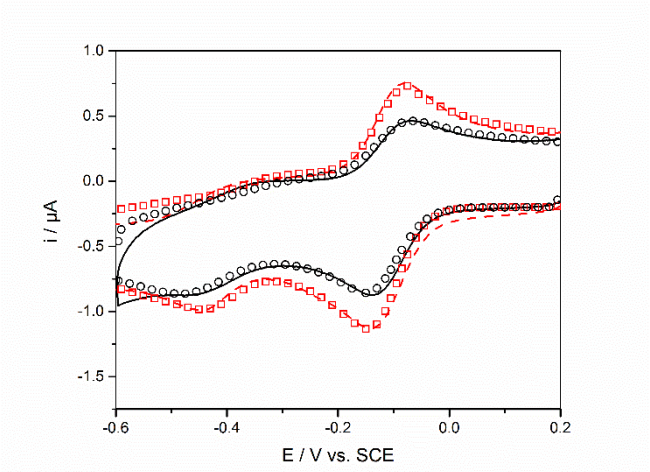

Figure 7. Cyclic voltammograms of TiPS-TPDO-tetraCN 2.10^{-4} M in MeCN + Bu_4NPF_6 0.1 M, on a Pt disk electrode (diameter 1.6 mm) at a scan rate of 100 mV s^{-1}, when water was introduced at a concentration of 1 M (dashed curve) and 2 M (solid line). The corresponding simulated curves of the 1 M (open squares) and 2 M (open circles) curves were calculated using scheme 2 with E^0_1 = - 0.113 V; k_{s1} = 0.04 cm s^{-1}; E^0_2 = - 0.49 V; k_{s2} = 0.01 cm s^{-1} ; E^0_3 = - 0.105 V; k_{s3} = 0.02 cm s^{-1}; k_{s4} = 0.02 cm s^{-1} ; K_1 = 0.3 ; k_{f1} = 15 s^{-1}; k_{f2} = 1 s^{-1}; K_3 = 0.5 M; k_{f3} = 0.06 M^{-1} s^{-1}; K_4 = 600 M; k_{f4} = 3 M^{-1} s^{-1}; K_5 = 1500 M ; k_{f5} = 2 M^{-1} s^{-1}; K_6 = 100; k_{f6} = 2560 s^{-1}; k_{fDISP} = 10 M^{-1} s^{-1}. In all electrochemical reactions, the transfer coefficient, α, was taken as 0.5, the diffusion coefficient was set at 10^{-5} cm^2 s^{-1} for all species and a resistance of 1 kΩ and a capacitance of 6 µF were introduced.

Films of vacuum evaporated TiPS-TPDO-tetraCN

We previously demonstrated[8] that films obtained by vacuum evaporated TiPS-TPDO-tetraCN lead to the formation of the diprotonated molecule. Fig. 8 depicts the absorption spectrum of a film of vacuum evaporated TiPS-TPDO-tetraCN deposited on an ITO electrode. Compared to that of TiPS-TPDO-tetraCN in solution (Fig. 3 and Table 1) or to that of a film deposed by spin coating,[8] additional bands appeared at 460, 585 and 638 nm which have been attributed to the diprotonated compound (TiPS-TPDO-tetraCN)H_2.[8] The reduced form is certainly stabilized in the solid-state via π-π interactions. Since the absorption bands of TiPS-TPDO-tetraCN were remained visible on the evaporated films, it can be suggested that TiPS-TPDO-tetraCN and (TiPS-TPDO-tetraCN)H_2 coexist in the solid-state. The charge transfer interactions could stabilized it as it was observed in the case of quinhydrone charge transfer complexes obtained from an equimolar mixture of quinone and dihydroquinone.[24] When the film was dissolved into CH_2Cl_2 (Fig. 8), the absorption spectrum evolved to lead to those of TiPS-TPDO-tetraCN (compare Fig. 3 and Fig. 8). In details, the bands attributed to (TiPS-TPDO-tetraCN)H_2 disappeared attesting the destruction of the diprotonated molecule.

The electrochemical behavior of the film was studied in aqueous solution according to pH.

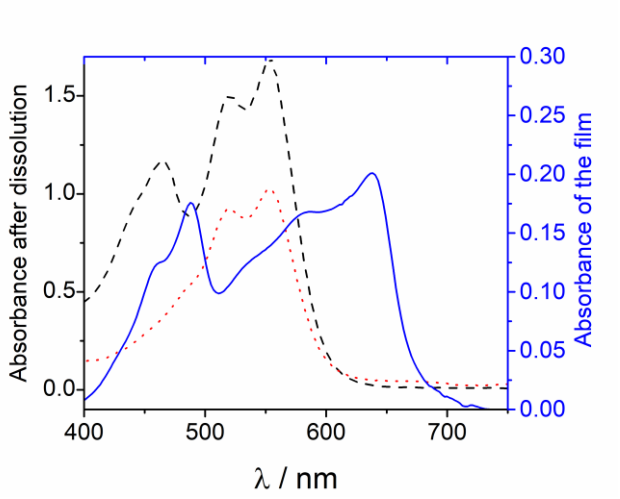

Figure 8. Absorption spectra of a film of vacuum evaporated TiPS-TPDO-tetraCN (50 nm) deposed on an ITO electrode dipped in a Britton-Robinson buffer (blue solid line) and of the same film immediately after its dissolution in CH_2Cl_2 (black dashed line) and after 3 days (red dotted line).

Degradation of the film occurred rapidly, therefore, a thin layer of nafion was dropped on the film. However, in that case, the anodic peak potentials were shifted towards more positive values compared to that obtained on the electrode without nafion, probably due to the low rate of transport of the counterions, whereas the cathodic ones remained unchanged. Therefore, only the cathodic peak potentials were reported according to pH (Fig. 9). From a mechanistic point of view, the reduction of TiPS-TPDO-tetraCN in aqueous medium involves an exchange of two electrons and one or two protons, according to pH. The mechanism can be described using a nine-member square scheme (Scheme 5).[11, 25] If the protonations are fast (at equilibrium), which is the case in buffered medium, the square scheme is kinetically equivalent to two successive reactions.[11, 25c]

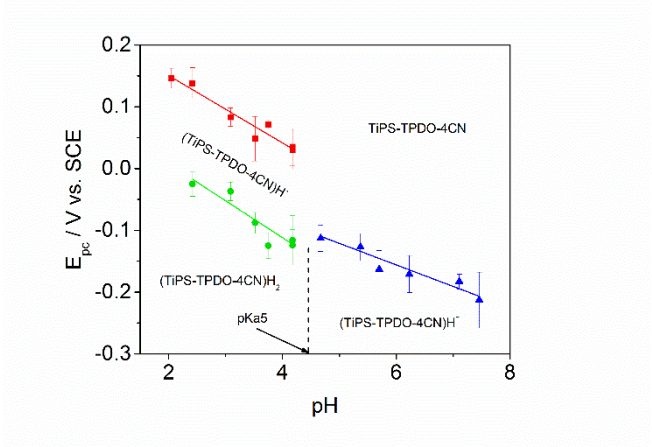

Figure 9. Variation of the cathodic peak potentials of an ITO electrode modified by a film of vacuum evaporated TiPS-TPDO-tetraCN according to pH. The electrode was dipped in a Britton Robinson buffer.

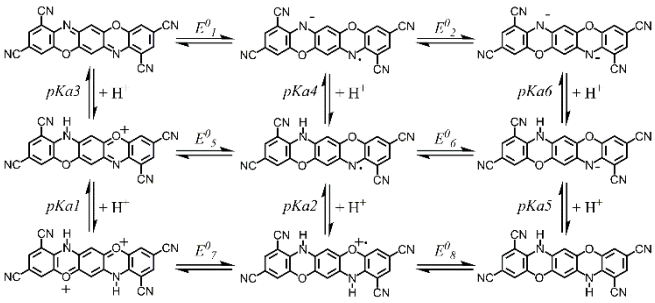

Scheme 5. The reaction scheme. In order to lighten the chemical formulae, TIPS groups have been omitted. The reductions are written horizontally from the left to the right and the protonations downwards. Indexing of potentials are different from those used by Laviron,[11, 25c] to be coherent with schemes 1 and 2.

The slopes of the graph E_{pc} = f(pH) (Fig. 9) define the number of protons involved during the reduction. For pH lower than 4.5, TiPS-TPDO-tetraCN was reduced in two successive one electron steps. The slopes of the straight lines were respectively -55 and -59 mV / pH unit, which indicates the uptake of one proton per electron. The first redox system has led to the protonated radical, which was then reduced in another ($1e^-$, $1H^+$) process yielding the fully protonated compound, (TiPS-TPDO-tetraCN)H_2. Above pH 4.5, the two stages overlapped and the process was equivalent to a simple $2e^-$ reaction with a slope equal to -34 mV / pH unit. It corresponds to a ($2e^-$, $1H^+$) process leading to the mono-protonated anion, (TiPS-TPDO-tetraCN)H^-. The changes in slopes at pH 4.5 correspond to pK_{a5} (Scheme 5). The evolution of the reduction of TIPS-TPDO-TetraCN as a function of pH provides another proof of TIPS-TPDO-TetraCNH_2 formation. Finally, the value of pK_{a5} is close to the pK_a one of aromatic amines, which justifies the chemical structure drawn in (Scheme 5).

Conclusions

The electrochemical reduction of TiPS-TPDO-tetraCN was studied both in solution and solid-state after vacuum evaporation on ITO electrodes. In CH_2Cl_2 solution, it occurs in two successive $1e^-$ reduction steps. But, in MeCN, the process is more complex: the intensity of the second system is lower than the first one and meanwhile a shoulder appears before the second cathodic peak. It has been attributed to the formation of a complex with water that facilitates the reduction of the radical anion. On the other hand, the spectroelectrochemical study demonstrated that the first $1e^-$ reduction leads to an equimolar mixture of the initial product, TiPS-TPDO-tetraCN, and a dianionic species (formed during the second reduction step). Firstly, it has been proven this result cannot stem from a DISP mechanism implicating only TPDO-type species ($E^0_1 > E^0_2$). Instead, a DISP reaction involving the radical anion and a counterpart molecule derived from structural changes to give back TiPS-TPDO-tetraCN and a restructured dianion has been successfully envisaged. Indeed, voltammograms which were simulated based on these mechanisms involving structural changes of the radical anion, a new DISP reaction and complexation with water, properly fit with the experimental results, even with different water concentrations.

Secondly, the study of TIPS-TPDO-teraCN thin films obtained by vacuum evaporation provides a proof that they are composed of diprotonated molecules. Indeed, the potential variations according to the pH showing that reduction occurs when pH < 4.5 in two successive ($1e^-$, $1H^+$) steps and above pH 4.5 in a single ($2e^-$, $1H^+$) stage were additional evidences of hydrogen-nitrogen bonds in evaporated TIPS-TPDOtetraCN materials. Moreover, this study has also made possible the experimental pK_a determination of the diprotonated compound (TiPS-TPDO-tetraCN)H_2.

Finally, we demonstrated that (TiPS-TPDO-tetraCN)H_2 is unstable and decomposes in solution while its straightforward formation in solid-state yields a stable material. $\pi-\pi$ and charge transfer interactions contribute to this stabilization as it was shown for the quinhydrone charge transfer complexes. Consequently, this study suggests that the active thin film coated in MSDI devices consists in a complex between diprotonated and unprotonated TIPS-TPDO-tetraCN. It brings a crucial element to understand the electronic properties of TPDO - based devices.

Experimental Section

Chemicals. All chemicals were used as received. Activated alumina, 2,2,6,6-tetramethyl-1-piperidinyloxy free radical (TEMPO) and tetrabutylammonium hexafluorophosphate (Bu_4NPF_6) were purchased from Sigma-Aldrich. Acetonitrile (MeCN, RPE) and CH_2Cl_2 (technical grade) were purchased from Carlo Erba. They were percolated on activated alumina. Britton-Robinson buffers (BR)[26] were prepared with acetic acid 99.7% (0.04 M), boric acid 99.99% (0.04 M) and phosphoric acid 99.999% (0.04 M) from Aldrich and with NaCl (0.2 M) from Carlo Erba as supporting electrolyte. The pH was adjusted to the desired value by addition of NaOH 1 M and distilled water. TiPS-tetracyanotriphenodioxazine (TiPS-TPDO-tetraCN) was synthesised according to a previously reported procedure.[6a] Thin films of TiPS-TPDO-tetraCN (50 nm) were prepared by sublimation under secondary vacuum (ca. 10^{-6} mbar) in a UNIVEX 250 thermal evaporator (Oerlikon, Germany),

at a rate of ca. 0.3 Å.s^{-1}, by heating in a temperature range of 320-350 °C, on Indium Tin Oxide (ITO) electrodes. For electrochemical experiments, a thin layer of nafion was deposed on the film and dried at 80 °C during one hour.

Electrochemistry. All electrochemical experiments were performed with a PGSTAT302 N (Metrohm) potentiostat connected to a PC and the data collected were analyzed using the Nova® 1.11 Software. Cyclic voltammetry (CV) was carried out by means of a three-electrode configuration consisting of the Pt disk (1.6 mm in diameter, Bioanalytical Systems) or the Indium Tin Oxide (ITO) modified electrode as working electrode, a platinum wire as counter-electrode and an SCE as reference. In organic solutions, the reference electrode was separated from the solution by a glass chamber with a porous vycor tip filled up with a saturated solution of Bu_4NPF_6 in the organic solvent (MeCN or CH_2Cl_2). Potentials were reported versus the saturated calomel electrode, SCE.

The working Pt electrode was soaked for 10 min in KOH (2 M), polished with 0.1 µm alumina, etched for 10 min in concentrated sulfuric acid (2 M) and sonicated 10 min in water, and then in absolute ethyl alcohol.

The solutions were deoxygenated for 10 min with argon, and a positive overpressure of argon was maintained above the electrolyte during the entire measurement performed at room temperature.

Digital simulations of cyclic voltammograms were simulated with DigiElch 8.

Spectroelectrochemistry. The in situ spectroelectrochemical experiments were performed with a BioLogic cell having an optical path of 1 mm. The working electrode was a Pt grid, the reference electrode an SCE and the counter electrode a Pt wire. The spectroelectrochemical experiments were carried out with a PGSTAT302 N (Metrohm) potentiostat. The spectra were recorded every 6 seconds by a UV-visible diode array spectrometer (KINSPEC II/MMS-16 VIS, BIOLOGIC) running in the kinetic mode with external trigger. The 150 W Xe lamp and the spectrometer were connected to the cell by optical fibers.

Computational chemistry. Molecular structures were optimized using density functional theory (DFT) at the B3LYP/6-31+G(d,p) level. Each structure was characterized as a minimum of the potential energy surface based on its real harmonic vibrational frequencies. Vertical excitation energies and excited state properties were determined using time-dependent (TD) DFT with the M06- 2X exchange-correlation functional (XCF) and the 6-311+G(d) basis set. This XCF was shown to provide good estimates of the transition energies of charge transfer states of medium and large-size organic molecules.[27] Solvent effects (acetonitrile) were included in all geometry optimizations and computations of optical properties by using the polarizable continuum model in its integral equation formalism (IEF-PCM).[28]

Acknowledgements

The authors acknowledge the Agence Nationale de la Recherche for funding through the projects CAP-BTX ANR-BLAN-2010-917-02, FMOCSOLE ANR-BLAN-2010-938-01 and OUTSMART ANR-2015-CE39-0004-03 and the MENESR for a PhD grant (A. W.). Financial support from the European Union (FEDER) and the Conseil Régional de Bourgogne through the FABER and the PARI SMT 08 and CDEA programs is gratefully acknowledged. We would like to thank the European Union for funding through the COST action TD1105 EuNetAir. The University of Bordeaux (G.G. PhD support), the CNRS and the institute of polytechnique of Bordeaux are acknowledged for financial support.

Keywords: TPDO • quinone diimine • square scheme • proton coupled electron transfer • disproportionation

[1] a) C. R. Newman, C. D. Frisbie, D. A. da Silva Filho, J.-L. Brédas, P. C. Ewbank, K. R. Mann, *Chem. Mater.* **2004**, *16*, 4436-4451; b) H. Usta, A. Facchetti, T. J. Marks, *Acc. Chem. Res.* **2011**, *44*, 501-510.

[2] a) Z. Bao, A. J. Lovinger, J. Brown, *J. Am. Chem. Soc.* **1998**, *120*, 207-208; b) R. Murdey, N. Sato, M. Bouvet, *Mol. Cryst. Liq. Cryst.* **2006**, *455*, 211-218.

[3] a) A. Facchetti, M.-H. Yoon, C. L. Stern, H. E. Katz, T. J. Marks, *Angew. Chem. Int. Ed.* **2003**, *42*, 3900-3903; b) T. M. Pappenfus, R. J. Chesterfield, C. D. Frisbie, K. R. Mann, J. Casado, J. D. Raff, L. L. Miller, *J. Am. Chem. Soc.* **2002**, *124*, 4184-4185.

[4] a) A. L. Briseno, S. C. B. Mannsfeld, C. Reese, J. M. Hancock, Y. Xiong, S. A. Jenekhe, Z. Bao, Y. Xia, *Nano Lett.* **2007**, *7*, 2847-2853; b) J. R. Ostrick, A. Dodabalapur, L. Torsi, A. J. Lovinger, E. W. Kwock, T. M. Miller, M. Galvin, M. Berggren, H. E. Katz, *J. Appl. Phys.* **1997**, *81*, 6804-6806.

[5] a) Z. Liang, Q. Tang, J. Xu, Q. Miao, *Adv. Mater.* **2011**, *23*, 1535-1539; b) F. Miao, *Synlett* **2012**, 326-336; c) X. Xiu, Y. Yao, B. Shan, X. Gu, D. Liu, J. Liu, J. Xu, N. Zhao, W. Hu, Q. Miao, *Adv. Mater.* **2016**, *28*, 5276-5283.

[6] a) G. Gruntz, H. Lee, L. Hirsch, F. Castet, T. Toupance, A. L. Briseno, Y. Nicolas, *Adv. Electron. Mater.* **2015**, *1*, 1500072-1500077; b) S. Jung, M. Albariqi, G. Gruntz, T. Al-Hathal, A. Peinado, E. Garcia-Caurel, Y. Nicolas, T. Toupance, Y. Bonnassieux, G. Horowitz, *ACS Appl. Mater. Interfaces* **2016**, *8*, 14701-14708.

[7] a) C.-a. Di, J. Li, G. Yu, Y. Xiao, Y. Guo, Y. Liu, X. Qian, D. Zhu, *Org. Lett.* **2008**, *10*, 3025-3028; b) Y. Nicolas, F. Castet, M. Devynck, P. Tardy, L. Hirsch, C. Labrugere, H. Allouchi, T. Toupance, *Org. Electron.* **2012**, *13*, 1392-1400.

[8] A. Wannebroucq, G. Gruntz, J.-M. Suisse, Y. Nicolas, R. Meunier-Prest, M. Mateos, T. Toupance, M. Bouvet, *Sens. Actuators B Chem.* **2018**, *255*, 1694-1700.

[9] A. Bolognese, C. Piscitelli, G. Scherillo, J. Org. Chem. 1983, 48, 3649-3652.

[10] M. L. Paddock, P. H. McPherson, G. Feher, M. Y. Okamura, Proc. Natl. Acad. Sci. U.S.A. 1990, 87, 6803-6807.

[11] E. Laviron, J. Electroanal. Chem. 1983, 146, 15-36.

[12] C. Lemmer, M. Bouvet, R. Meunier-Prest, Phys. Chem. Chem. Phys. 2011, 13, 13327-13332.

[13] C. Liehn, M. Bouvet, R. Meunier-Prest, ChemElectroChem. 2014, 1, 2116-2123.

[14] a) M. Bouvet, B. Malézieux, P. Herson, Chem. Commun. 2006, 1751-1753; b) T. Sakurai, Acta Crystallogr. 1965, 19, 320-330.

[15] D. H. Evans, M. W. Lehmann, Acta Chem. Scand. 1999, 53, 765-774.

[16] F. Barrière, W. E. Geiger, J. Am. Chem. Soc. 2006, 128, 3980-3989.

[17] a) R. J. Forster, T. E. Keyes, M. Farrell, D. O'Hanlon, Langmuir 2000, 16, 9871-9877; b) N. Gupta, H. Linschitz, J. Am. Chem. Soc. 1997, 119, 6384-6391; c) Y. H. Hui, E. L. K. Chng, C. Y. L. Chng, H. L. Poh, R. D. Webster, J. Am. Chem. Soc. 2009, 131, 1523-1534; d) Z. H. Lim, E. L. K. Chng, Y. L. Hui, R. D. Webster, J. Phys. Chem. B 2013, 117, 2396-2402; e) M. Quan, D. Sanchez, M. F. Wasylkiw, D. K. Smith, J. Am. Chem. Soc. 2007, 129, 12847-12856.

[18] a) M. Mastragostino, L. Nadjo, J. M. Saveant, Electrochim. Acta 1968, 13, 721-749; b) J. M. Saveant, Elements of Molecular and Biomolecular Electrochemistry: An Electrochemical Approach to Electron Transfer Chemistry, John Wiley & Sons, Hoboken, New Jersey, 2006.

[19] a) J. Sobek, R. Martschke, H. Fischer, J. Am. Chem. Soc. 2001, 123, 2849-2857; b) P. J. Wright, A. M. English, J. Am. Chem. Soc. 2003, 125, 8655-8665.
[20] M. Shimizu, Y. Asai, Y. Takeda, A. Yamatani, T. Hiyama, Tetrahedron Lett. 2011, 52, 4084-4089.
[21] T. Takeda, H. Sugihara, Y. Suzuki, J. Kawamata, T. Akutagawa, J. Org. Chem. 2014, 79, 9669-9677.
[22] a) D. H. Evans, Chem. Rev. 1990, 90, 739-751; b) N. A. Macías-Ruvalcaba, D. H. Evans, J. Phys. Chem. B 2006, 110, 5155-5160.
[23] K. Hunger, R. Hamprecht, P. Miederer, C. Heid, A. Engel, K. Kunde, W. Mennicke, J. Griffiths, in Industrial Dyes, Wiley-VCH Verlag GmbH & Co. KGaA, 2004, pp. 113-338.
[24] M. Bouvet, B. Malezieux, P. Herson, F. Villain, CrystEngComm 2007, 9, 270-272.
[25] a) E. Laviron, J. Electroanal. Chem. 1984, 169, 29-46; b) E. Laviron, R. Meunier-Prest, J. Electroanal. Chem. 1992, 324, 1-18; c) R. Meunier-Prest, E. Laviron, J. Electroanal. Chem. 1992, 328, 33-46.
[26] H. T. S. Britton, R. A. Robinson, J. Chem. Soc. 1931, 1456-1462.
[27] a) K. Brymora, L. Ducasse, A. Delaure, L. Hirsch, T. Jarrosson, C. Niebel, F. Serein-Spirau, R. Peresutti, O. Dautel, F. Castet, Dyes Pigm. 2018, 149, 882-892; b) D. Jacquemin, E. A. Perpète, I. Ciofini, C. Adamo, R. Valero, Y. Zhao, D. G. Truhlar, J. Chem. Theory Comput. 2010, 6, 2071-2085.
[28] J. Tomasi, B. Mennucci, R. Cammi, Chem. Rev. 2005, 105, 2999-3094.